The 12th International Conference of
International Association for Computer Methods and Advances in Geomechanics (IACMAG)
1-6 October, 2008
Goa, India

Finite Element Investigation of Base Tilt Effect on Shallow Foundation Collapse

J.M.M.C. Marques
Dept. of Civil Engineering, Faculty of Engineering, University of Porto, Porto, Portugal

R.N.T. Teixeira
Dept. of Civil Engineering, Swansea University, Swansea, U.K.

Keywords: bearing capacity, shallow foundations, base tilt, finite element modelling.

ABSTRACT: The bearing capacity of shallow foundations is classically computed as the sum of three contributions, coming from the soil cohesion, the overburden pressure and the weight of the soil mass mobilized by the collapse mechanism. Each of these contributive terms is then multiplied by several special corrective factors that account for the effect of the shape, depth and tilt of the foundation base, the inclination and eccentricity of the applied load, as well as the slope of the ground. Formulas for such factors have been proposed by several authors and are adopted by many codes of practice, namely Eurocode 7. This paper presents a numerical investigation of the adequacy and range of validity of the corrective factors that apply to foundation base tilt. Tilt angles of 6 and 9 degrees, rigid and flexible footings and small and large strain formulations are combined in a total of 8 finite element analyses of shallow foundation collapse in undrained conditions. It is concluded that for tilt angles above 6º the bearing capacity tends to be overestimated by the classical approach which may lead to estimates that are not on the safe side.

1 Introduction

Geotechnical Engineering is probably the area within Civil Engineering where displacements and strains of considerable magnitude occur more frequently, not only during construction and normal service conditions, but also in the case of collapse. The large displacements associated with consolidation phenomena and the finite strains in slope failure surfaces are familiar examples.

The consideration of geometric nonlinearity in the finite element modelling of shallow foundation collapse helps to get a better grasp of the physics of the problem, as will be shown by a numerical study.

This paper focuses on the appropriateness of the corrective factors associated with the tilt of the foundation base, extending previous work dedicated to shallow foundation collapse (Marques and Teixeira, 2002; Marques and Teixeira, 2007). In engineering practice tilted foundation bases are frequently adopted in gabion retaining wall design.

2 Bearing capacity of shallow foundations

The bearing capacity of shallow foundations has been studied by Prandtl, Terzaghi (1943), Meyerhof (1963), Brinch Hansen (1970), Vesic (1973), Skempton and other illustrious scholars. The design procedure currently embodied in codes of practice, such as Eurocode 7 (2004), has evolved from those pioneering contributions. The bearing capacity is computed as the sum of three terms, respectively due to soil cohesion, weight of the overburden and weight of the soil mass mobilized by the collapse mechanism.

In the basic case, depicted in Figure 1, of a flexible strip footing with horizontal base of width B, at depth D in a homogeneous and horizontal soil stratum with unit weight g, cohesion c' and friction angle f', under the action of a vertical, centred load Q, the bearing capacity q_{ult} is given by:

$$q_{ult} = Q_{ult} / B = c' N_c + \overline{q} N_q + 1/2 B g N_g \quad (1)$$

The bearing capacity factors N_c, N_q and N_g are defined as (Vesic, 1975):

$$N_c = \left(N_q - 1\right) \Big/ \tan f' \qquad N_q = e^{p \tan f'} \tan^2\left(p/4 + f'/2\right) \qquad N_g = 2\left(N_q - 1\right)\tan f' \qquad (2)$$

For the case of purely cohesive soils ($f' = 0$) the value of N_c is $p + 2$.
The soil layer of thickness D above the footing base level is considered as a surcharge, $\bar{q} = g\,D$, its shearing resistance being neglected in Equation 1 in this basic case illustrated in Figure 1.

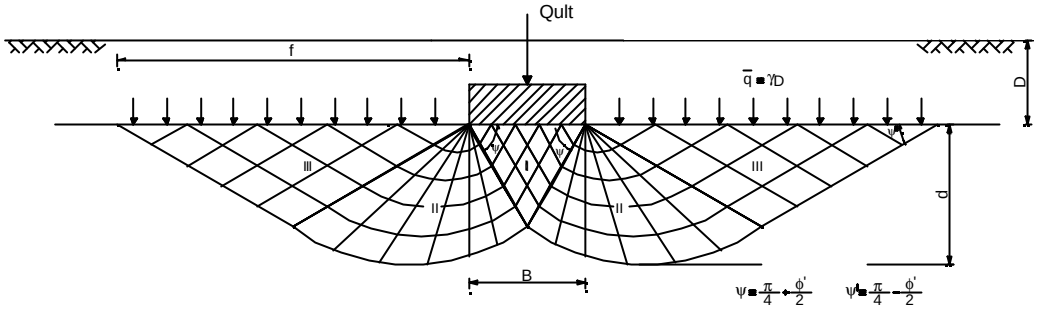

Figure 1. Failure mechanism of a shallow strip footing.

Each of the three terms on the right hand side of Equation 1 may be extended to include several specific corrective factors, in order to account for the effect of the shape, depth and tilt of the foundation base, the inclination and eccentricity of the applied load, as well as the slope of the ground, to name but a few of the possible deviations from the basic case of Figure 1.

This paper presents a finite element investigation of the adequacy and range of validity of the corrective factors that pertain to the case of foundation base tilt, illustrating the corresponding failure pattern. Undrained conditions have been considered. One complementary aspect of this study is the comparison of results obtained with both small strain and large strain formulations, which provides an interesting insight into the physics of the failure process.

3 Effect of foundation base tilt

When the base of the footing makes an angle a with respect to the horizontal, the corrective factors b_c, b_q and b_g are introduced in Equation 1:

$$q_{ult} = Q_{ult}/B = c' N_c b_c + \bar{q}\, N_q b_q + 1/2\, B g N_g b_g \qquad (3)$$

Those corrective factors are given by (Vesic, 1975):

$$b_c = b_q - \left(1 - b_q\right)\Big/\left(N_c \tan f'\right) \qquad b_q = b_g = \left(1 - a \tan f'\right)^2 \qquad (4)$$

In the case of purely cohesive soils ($f' = 0$) we have for b_c (with a in radians)

$$b_c = 1 - \left[2a/\left(p + 2\right)\right] \qquad (5)$$

4 Effect of the shearing resistance of the overburden

The contribution to the bearing capacity due to the shearing resistance of the soil layer above the base of the footing may be accounted for by introducing in Equations 1 and 3 the following depth corrective factors d_c, d_q and d_g, proposed by Brinch Hansen (1970) for the case of $D/B \le 1$:

$$d_c = d_q - \left(1 - d_q\right)\Big/\left(N_c \tan f'\right) \qquad d_q = 1 + 2\tan f' \left(1 - \sin f'\right)^2 D/B \qquad d_g = 1 \qquad (6)$$

In the case of $f' = 0$ we have for d_c

$$d_c = 1 + 2D\Big/\left[\left(p + 2\right) B\right] \approx 1 + 0.4\, D/B \qquad (7)$$

The depth corrective factors will be used to investigate the effect on the bearing capacity of the progressive embedment of the footing into the foundation soil as the applied load is incremented.

5 Numerical study

In order to isolate as much as possible the effect of the base tilt on the bearing capacity an undrained scenario

has been selected, with the footing resting at the soil surface. In this way we have $c' = c_u$, $f' = 0$, $\bar{q} = gD = 0$ and consequently only the first term on the right hand side of Equation 3 is non-zero, the bearing capacity being given by:

$$q_{ult} = Q_{ult}/B = c_u N_c b_c = c_u (p+2)\left\{1-\left[2a/(p+2)\right]\right\} = c_u (p+2-2a) \quad (8)$$

Three components have been contemplated in this numerical study:

(i) Tilt angle magnitude – Values of 6° and 9° were selected for a. Two 8-noded element meshes were prepared and the one for the lower tilt value is shown in Figure 2. Both meshes have 951 elements and 2994 nodes, with the lateral and bottom boundary nodes on rollers. The soil properties adopted are E = 12MPa, n = 0.49 and c_u = 30kPa. The Tresca law has been used. The strip footing width is $B = B'/\cos a$, with B' = 14 m.

(ii) Footing stiffness – The two theoretical limit cases, flexible footing and rigid footing, have been considered. The flexible footing corresponds to the application of a uniformly distributed vertical stress at the soil surface on the foundation footprint. Load incrementation is controlled by an arc-length algorithm.

The rigid footing has been materialized by the inclusion of 36 additional finite elements whose E value is 1000 times that of the soil. An increasing vertical displacement was imposed to the central node at the top of the short column that emerges from the footing (see Figure 2). In this way the footing is left free to rotate clockwise as soil yielding develops around its right corner. The alternative of imposing vertical displacements on the foundation footprint soil nodes would have prevented rotation from occurring, leading to a presumably stiffer and unrealistic response.

(iii) Geometric nonlinearity – Small strain and large strain analyses were conducted. The consideration of geometrical nonlinearity in the form of an updated lagrangian procedure allows for the progressive embedment of the footing into the soil to be taken into account. The gradually increasing contribution of the shearing resistance of the soil above the footing base as it moves downwards can be tentatively estimated by including in Equation 8 the depth corrective factor of Equation 7:

$$q_{ult} = Q_{ult}/B = c_u N_c b_c d_c = c_u (p+2-2a)(1+0.4D/B) \quad (9)$$

In the base tilted case only one half is developed of the symmetric failure mechanism of Figure 1, as will be shown later on. It seemed thus reasonable to adopt for the embedment depth, D, in Equation 9, the magnitude of the vertical displacement at the centre of the footing base, which is roughly one half of that of its rightmost node.

By exploring these three alternative options a total of eight analyses have therefore been performed.

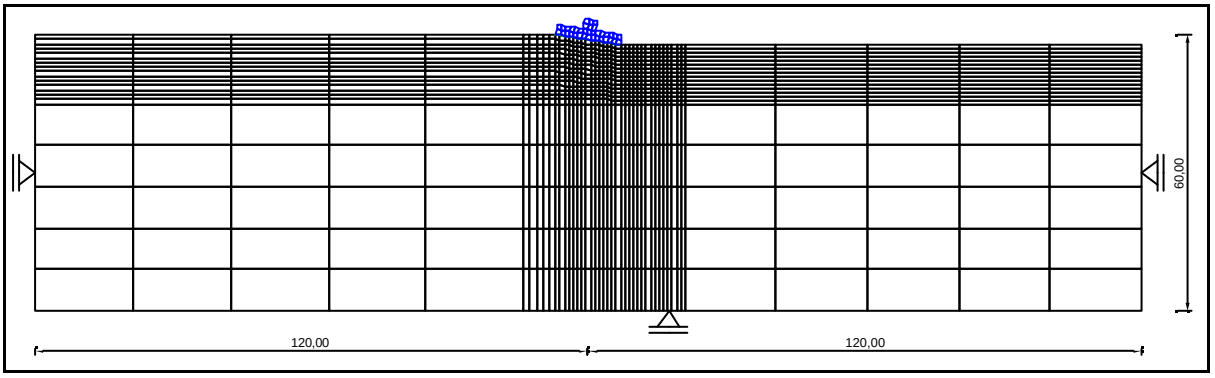

Figure 2. Finite element mesh for α=6°.

5.1 Small strain results

Figure 3 shows the curves obtained with the small strain formulation for the normalized load-displacement response, where the vertical displacement d_y at the base centre is divided by the footing width B, while the applied vertical pressure q is divided by c_u. In the rigid footing case an average value for q is obtained from $q=R/B$, where R is the vertical reaction force at the node where the downward displacement is incrementally prescribed.

For the case of α=6° the results of the rigid and flexible analyses lie respectively above and below the

analytical solution extracted from Equation 8, whereas for α=9° the analytical solution seems to overestimate the bearing capacity, especially in the flexible footing case.

5.2 Large strain results

The large strain plots of Figure 4 present a hardening branch that corresponds to the additional bearing capacity brought in by the shearing resistance of the progressively thicker soil layer lying above and to the right of the sinking footing base.

The "analytical solution" has been obtained in this case from Equation 9 with *D* chosen according to the criterion described above. Once more there is good agreement for α=6°, while for α=9° the numerically computed bearing capacity falls again below that predicted by the classical formula.

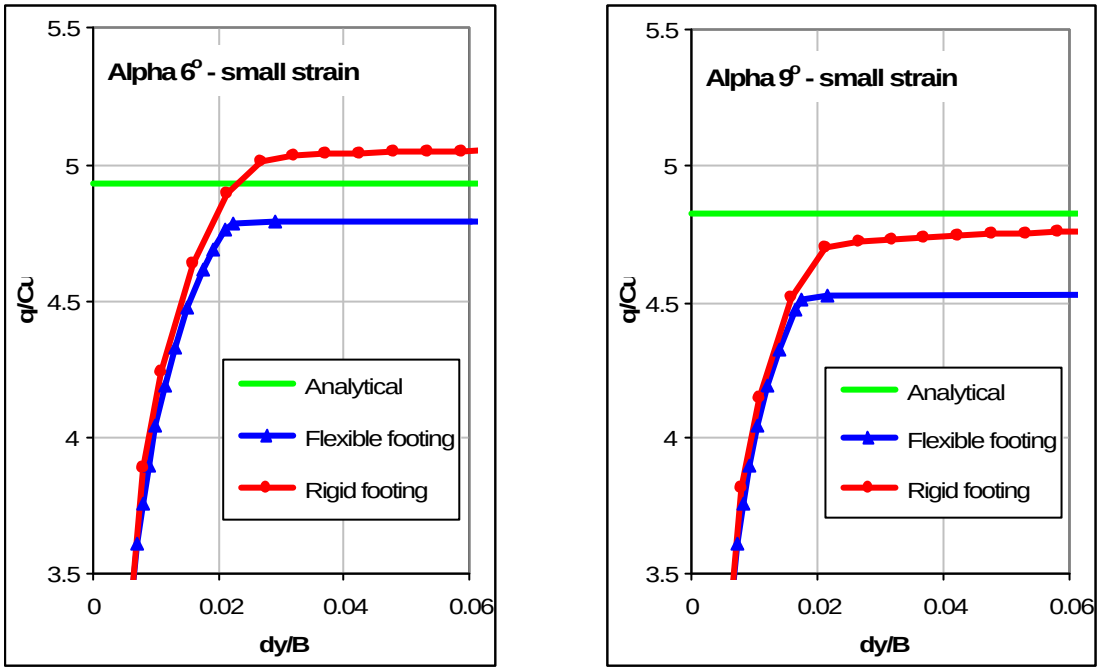

Figure 3. Small strain results.

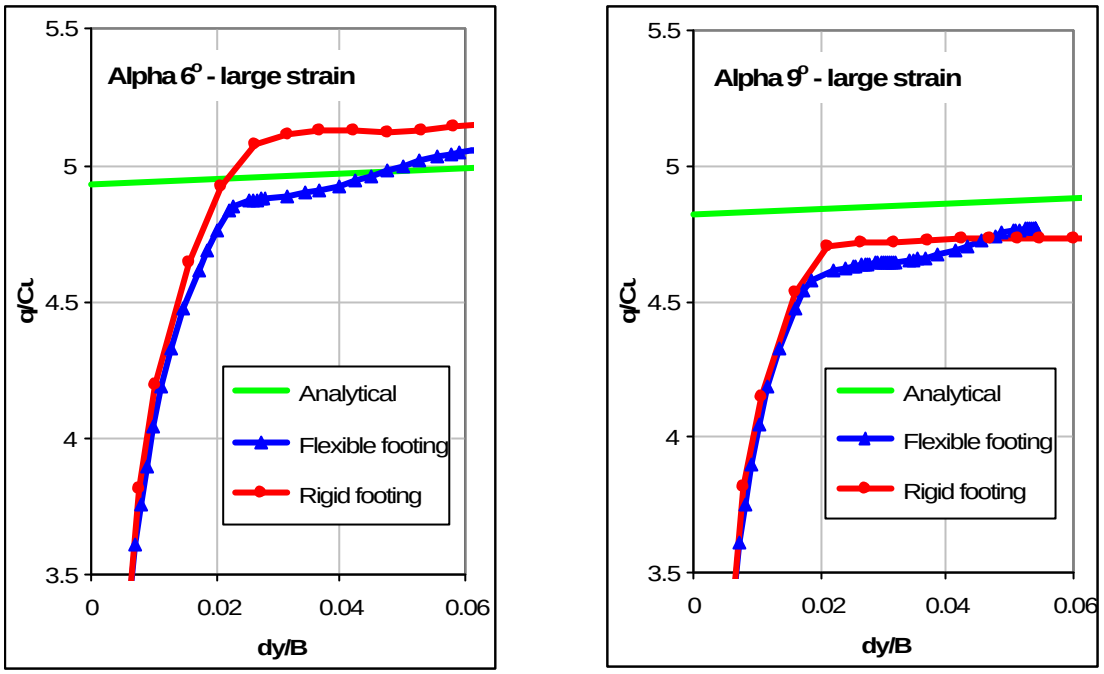

Figure 4. Large strain results.

Figures 5 and 6 present large strain results for the rigid footing with α=6° and α=9°, respectively, while Figures 7 and 8 cover the flexible footing with α=6° and α=9°. Each Figure displays effective plastic strain, deformed mesh, displacement magnitude $(d_x^2+d_y^2)^{½}$ and nodal vector plots. The flexible footing plots were extracted from results obtained with coarser meshes than that of Figure 2.

The clockwise rotation and the horizontal displacement component of the rigid footing can be fully appreciated in the vector plots.

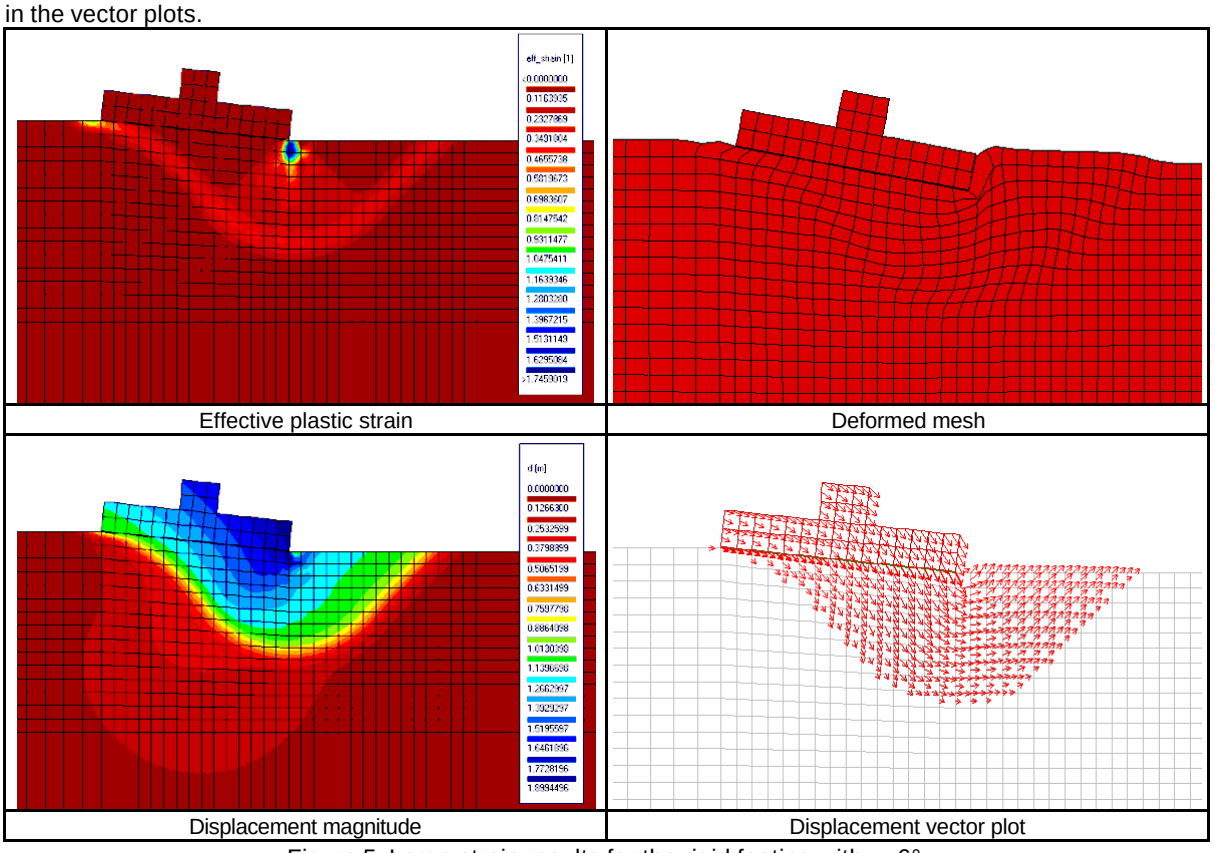

Figure 5. Large strain results for the rigid footing with α=6°.

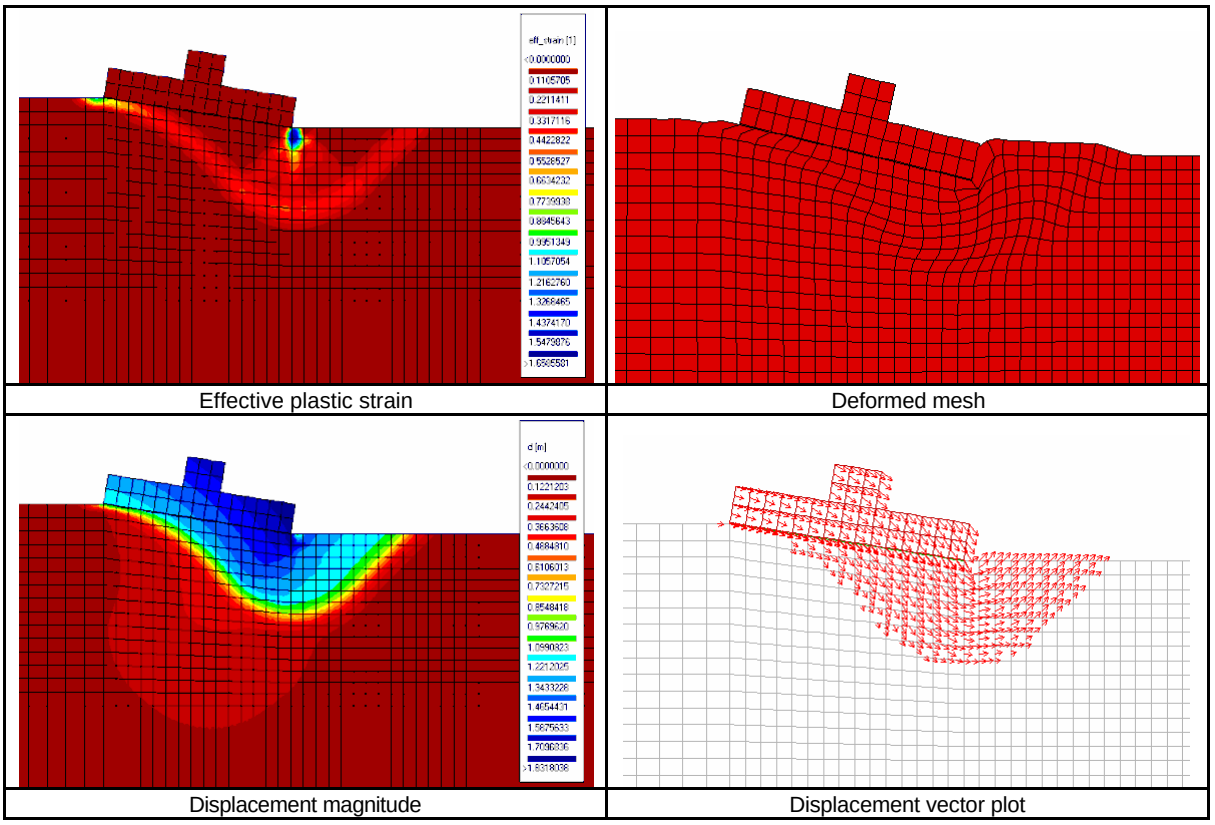

Effective plastic strain | Deformed mesh

Displacement magnitude | Displacement vector plot

Figure 6. Large strain results for the rigid footing with α=9°.

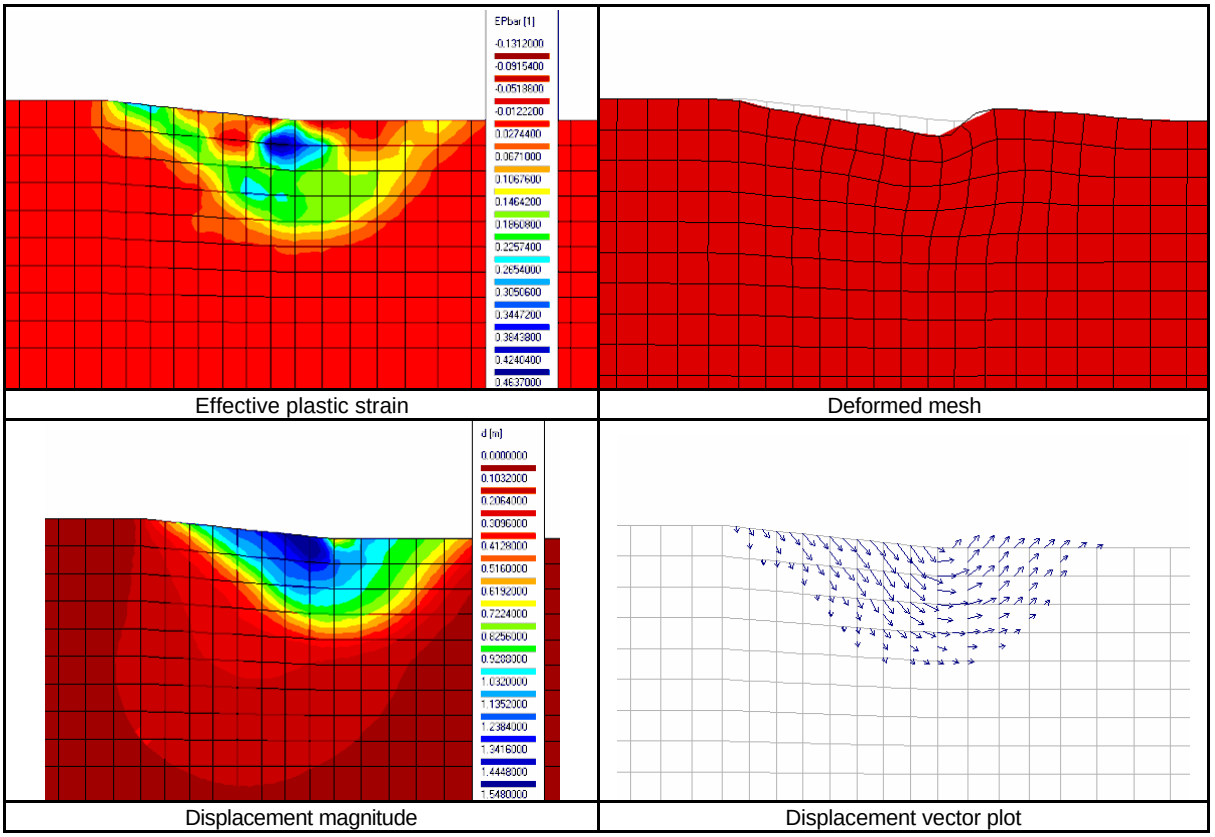

Effective plastic strain | Deformed mesh

Displacement magnitude | Displacement vector plot

Figure 7. Large strain results for the flexible footing with α=6°.

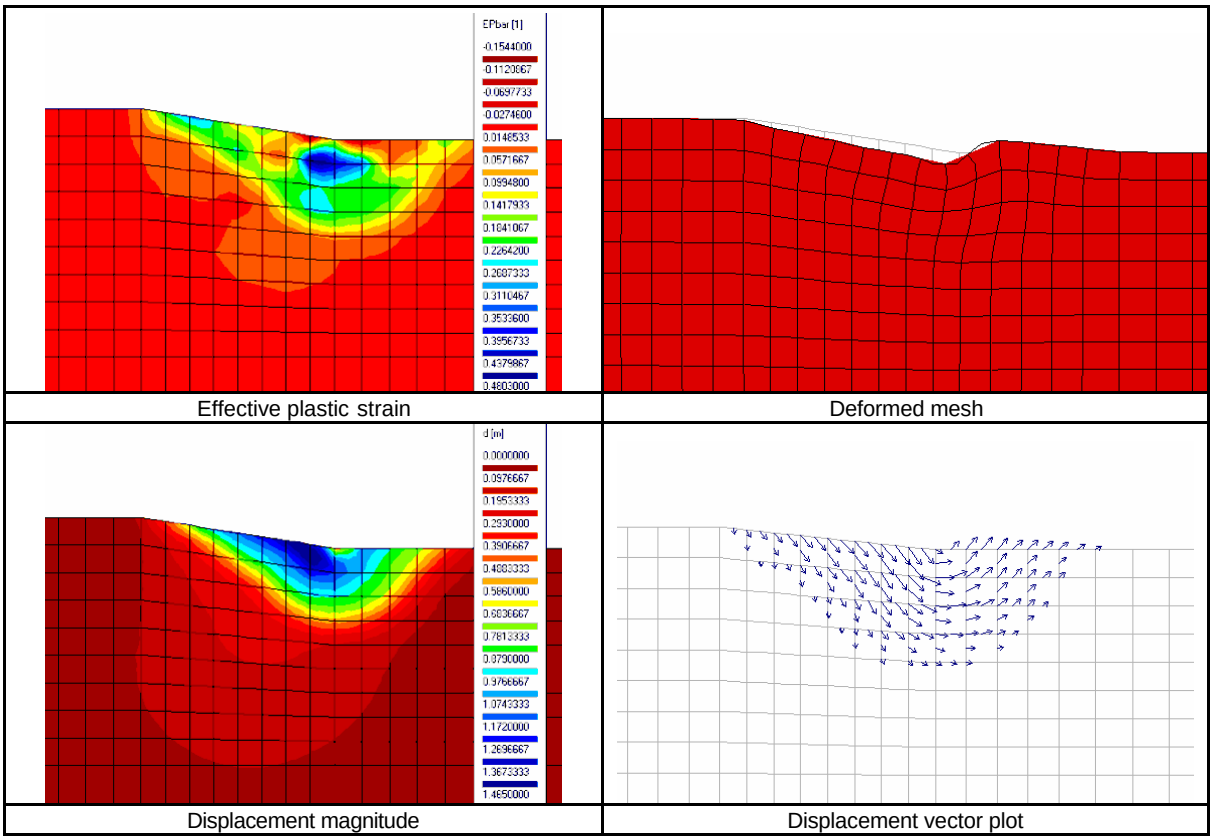

Figure 8. Large strain results for the flexible footing with α=9°.

The effective strain plots show that the shape of the collapse mechanism is approximately one half of that depicted in Figure 1, extending to the right of the footing. The displacement vector plots confirm the localised nature of the collapse mechanism.

The rigid footing analyses have encountered some convergence difficulties in spite of being displacement driven. This fact was due to the very large deformation and yielding of the soil element adjacent to the right edge of the footing base, as shown by the deformed meshes and by the blue zone on the effective plastic strain plots of Figures 5 and 6.

6 Conclusions

The objective of this paper was to assess the validity of the corrective factors proposed in the literature and adopted in Eurocode 7 that account for effect of the tilt of the foundation base in the bearing capacity calculation of shallow foundations. A set of 8 finite element analyses has been performed with two tilt angles, rigid and flexible footings and small and large strain formulations. It has been concluded that for tilt angles above 6° the classical approach tends to overestimate the bearing capacity.

7 References

Brinch Hansen J. 1970. A revised and extended formula for bearing capacity, *Danish Geotechnical Institute,* **28**, 5-11.

EN 1999-1, Eurocode 7: Geotechnical design – Part 1: General rules. 2004. CEN, Brussels (Belgium).

Marques J.M.M.C. and Teixeira R.N.T. 2002. Geometrically non-linear modelling of shallow foundation collapse (in Portuguese), Proc. 8º Congresso Nacional de Geotecnia, Lisbon (Portugal), 885-894.

Marques J.M.M.C. and Teixeira R.N.T. 2007. Geometrically non-linear modelling of shallow foundation collapse on sloping ground, *Computational Plasticity IX*, Oñate E. et al. (Eds.), CIMNE, Barcelona (Spain), 312-315.

Meyerhof G.G. 1963. Some recent research on the bearing capacity of foundations, *Canadian Geotechnical Journal*, **1**, 16-26.

Terzaghi K. 1943. *Theoretical Soil Mechanics*, Wiley, New York (USA).

Vesic A.S. 1973. Analysis of ultimate loads of shallow foundations, *J. Soil Mech. Found. Division, ASCE,* **99**, 45-73.

Vesic A.S. 1975. Bearing capacity of shallow foundations, Chapter 3, *Foundation Engineering Handbook*, Winterkorn H.F. and Fang H.-Y. (Eds.), Van Nostrand Reinhold, New York (USA).